Acta of Bioengineering and Biomechanics
Vol. 21, No. 3, 2019

Original paper
DOI: 10.5277/ABB-01401-2019-02

Bone conduction stimulation of the otic capsule: a finite element model of the temporal bone

PAWEŁ BORKOWSKI[1]*, PIOTR MAREK[1], KAZIMIERZ NIEMCZYK[2], MAGDALENA LACHOWSKA[2], MONIKA KWACZ[3], JAROSŁAW WYSOCKI[4]

[1] Warsaw University of Technology, Faculty of Power and Aeronautical Engineering, Institute of Aeronautics and Applied Mechanics, Warsaw, Poland.
[2] Medical University of Warsaw, Department of Otolaryngology, Warsaw, Poland.
[3] Warsaw University of Technology, Faculty of Mechatronics, Institute of Micromechanics and Photonics, Warsaw, Poland.
[4] Lazarski University, Medical Faculty, Warsaw, Poland.

Purpose: Bone conduction stimulation applied on the otic capsule may be used in a conductive hearing loss treatment as an alternative to the bone conduction implants in clinical practice. A finite element study was used to evaluate the force amplitude and direction needed for the stimulation. *Methods*: A finite element model of a female temporal bone with a precisely reconstructed cochlea was subjected to a harmonic analysis assuming two types of stimulation. At first, the displacement amplitude in the form of air conduction stimulation was applied on the stapes footplate. Then the force amplitude was applied on the otic capsule in the form of bone conduction stimulation. The two force directions were considered: 1) the primary direction, when a typical opening is performed during mastoidectomy, and was coincident with the axis of an imaginary cone, inscribed in the opening, and 2) the direction perpendicular to the stapes footplate. The force amplitude was set so that the response from the cochlea corresponded to the result of air conduction stimulation applied on the stapes footplate. *Results*: The amplitude and phase of vibration and the volume displacement on the round window membrane were considered as well as vibrations of the basilar membrane, spiral lamina, and promontory. *Conclusions*: The cochlear response was comparable for the two types of stimulation. The efficiency of bone conduction stimulation depended on the force direction. For the primary direction, the force was a few times smaller than for the direction perpendicular to the stapes footplate.

Key words: *bone conduction, finite element analysis, temporal bone, otic capsule, cochlea, inner ear*

1. Introduction

The effectiveness of ear stimulation by bone conduction (BC) depends on a type and position of a stimulator, as it was shown in experimental tests. Håkansson et al. [11] observed an increased promontory acceleration for a smaller distance between the otic capsule and BC implant. The results of research by Eeg-Olofsson et al. [3] indicated that hearing perception from BC sound can be correlated with the vibration of the otic capsule, induced by the bone-anchored hearing systems (BAHS), located on the squamous part. Experimental studies were also carried out on the inner ear to investigate vibrations of the round window (RW) membrane and the stapes footplate (SF) as well as vibrations of the basilar membrane (BM) and the spiral lamina (SL) for the air and bone conduction pathways [1], [24], [25], [26].

In addition to experimental studies, the BC phenomenon was also modeled numerically by using the finite element (FE) method. The model by Chang et al. [2], including the entire head, did not contain detailed description of the inner ear, because its purpose was to identify the role of different tissues in the vibration transmission. The isolated external, middle, or inner ear structures were numerically modeled to investigate the physics of sound transmission [5], [6], implants of

* Corresponding author: Paweł Borkowski, Warsaw University of Technology, Faculty of Power and Aeronautical Engineering, Institute of Aeronautics and Applied Mechanics, ul. Nowowiejska 24, 00-665 Warsaw, Poland. Phone: +48 22 234 79 92, fax. +48 22 234 74 48, email: pbork@meil.pw.edu.pl

Received: June 8th, 2019
Accepted for publication: July 17th, 2019

the stapes [13], [14], and a transducer for the RW stimulation [18].

The purpose of this FE study was to investigate the effectiveness of direct BC stimulation applied on the otic capsule, which may be used in a conductive hearing loss treatment as an alternative to the BAHS or other bone conduction implants. The results of numerical simulation aimed to answer questions: what is the value of force needed for BC stimulation applied on the otic capsule, and whether the direction of stimulation is an important factor for BC stimulation.

2. Materials and methods

2.1. FE model

The right temporal bone of a 25-year-old woman was scanned using the computer tomography (CT) (Fig. 1a) and processed in the ScanIp software (Synopsys Inc., Mountain View, California, United States). The resulting *iges* file contained the surface of compact bone described by triangular surfaces with the edge length of 0.5 mm. The inner ear was scanned at a higher resolution, and the edge size was 0.05 mm. The geometry was then processed using the ANSYS program (ANSYS Inc., Canonsburg, Pennsylvania, United States). The temporal bone was divided into cortical and trabecular part, and the air cells were neglected (Fig. 1b). The otic capsule surrounded the cochlea of nearly anatomical shape (Fig. 2e).

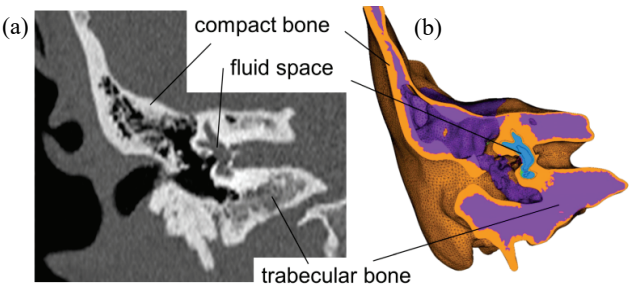

Fig. 1. The frontal cross-section of the temporal bone: (a) an image from the computer tomography, (b) similar view of the finite element (FE) model

When creating a geometric model, points in the selected cross-sections were used to create spline curves. Surfaces were interpolated using Coon's path, and volumes were created. The inner ear geometry was represented by the set of volumes to create a hexahedral FE mesh, particularly at the interface between the fluid and solid tissues. Except for the cochlea, the temporal bone was discretized by tetrahedral FEs. The temporal bone and the inner ear were described by over 12 000 areas

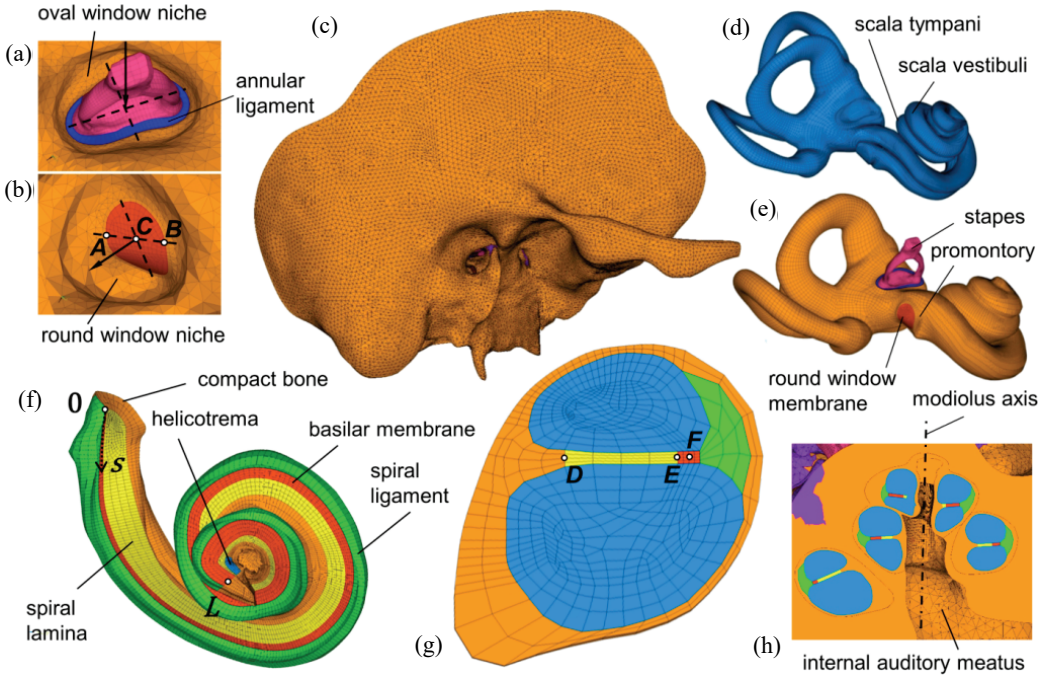

Fig. 2. Finite element (FE) model of the right temporal bone; (a) the oval window with axes, (b) the round window (RW) membrane and its normal direction: points A and B – mark surrounding bone, point C – marks the center, (c) lateral view, (d) fluid space of the cochlea, (e) the bony labirynth and the stapes, (f) interior of the cochlea and coordinate s (0, L), (g) cross section through one of the turns of the cochlea with marked characteristic points: D – base of the spiral lamina (SL), E – edge of the spiral lamina (SL), F – center of the basilar membrane (BM), (h) cross-section of the cochlea

and about two thousand volumes. The FE model consisted of about 560 000 nodes and almost two million FEs (Fig. 2c). The outer surface of the bone was covered by FEs with the added mass per unit area imitating soft tissues and the brain fluid near the bone.

Displacements in solid tissues and nodal pressures in the fluid were calculated numerically using the FE method. For the solid structures, a set of equations representing the equation of motion of a discrete system was considered (Eq. (1)):

$$[M]\frac{d^2\{u(t)\}}{dt^2}+[C]\frac{d\{u(t)\}}{dt}+[K]\{u(t)\}=\{F(f,t)\}, \tag{1}$$

where the left side was the sum of the mass matrix multiplied by the vector of nodal accelerations, the damping matrix multiplied by the nodal velocity vector, and the stiffness matrix multiplied by the nodal displacement vector. The right side was represented by the vector of nodal load applied as a harmonic function of frequency and time. A lossy acoustic wave equation without mass sources was considered for the fluid (Eq. (2)):

$$\nabla^2 px,y,z,t)-\frac{1}{c^2}\frac{\partial^2 p}{\partial t^2}+\frac{4\mu}{3\rho_0 c^2}\nabla^2\frac{\partial p}{\partial t}=0;\quad c=\sqrt{\frac{K}{\rho_0}}, \tag{2}$$

which contained the Laplacian of acoustic pressure with respect to Cartesian coordinates, the second derivative of pressure over time divided by the sound velocity squared, and additional component including viscosity of the fluid and the Laplacian of the first derivative of pressure over time. The sound velocity was calculated as a square root of the bulk modulus per mean fluid density. The coupling of the fluid and structure displacements in the direction normal to the interface was assumed, including the sound absorption applied as the boundary admittance (Eq. (3)), and equilibrium of stress in the structure and the fluid pressure at the interface (Eq. (4)).

$$\vec{n}\cdot\vec{u}_S-\vec{n}\cdot\vec{u}_F=-j\frac{Y}{2\pi f}p;\quad j=\sqrt{-1}, \tag{3}$$

$$\sigma\cdot\vec{n}+p\cdot\vec{n}=\vec{0}. \tag{4}$$

To imitate the air conduction (AC) pathway due to vibrations of the eardrum, the harmonic displacement and rotations were applied at the SF. For BC stimulation, a harmonic force was applied on the mass element attached to the otic capsule. Therefore, BC stimulation was parameterized in terms of space, amplitude, direction, and frequency.

2.2. Properties of tissues

Solid tissues in the presented FE model were assumed as isotropic, and some linear elastic and viscoelastic properties were defined as functions of position and frequency. The assumption about linearity enabled scaling the results to compare effects of AC and BC stimulation.

The skull bone consists of the external and internal plates of compact bone separated by the layer of trabecular bone. The properties of compact bone, like the degree of anisotropy and direction of the maximum stiffness axis depend on site. The external and internal layers have different thickness and stiffness [20]. In dynamic tests, compact bone exhibited viscoelastic properties depending on strain rate [12], [17]. In a human temporal bone, the internal compact plate covers the petrous part and the diploe is replaced by the tympanic cavity and air cells. Due to the structure complexity, the compact bone was assumed as isotropic and viscoelastic. The storage E_c' and loss E_c'' moduli (Eqs. (5), (6)) were dependent on the frequency f (Hz).

$$E_c' = 369\cdot\ln(f)+9628\ (\text{MPa}), \tag{5}$$

$$E_c'' = 26.15\cdot f^{0.308}\ \ (\text{MPa}). \tag{6}$$

The above data were based on experimental measurements of human femoral bones [17]. In the presented model, the thickness of cortical bone depended on site (Fig. 1).

Dynamic properties of trabecular bone strongly depend on the tissue density [16], [19]. In the experimental test conducted at low frequencies, the storage modulus and the loss factor were almost constant [21]. In the presented model, the density of trabecular bone was defined as the average value of the range measured by Ouyang et al. [19]. The constant stiffness of trabecular bone was assumed, and the structural damping was defined as a linear function of frequency based on the experimental data [21] and tuned for the entire frequency range using the FE model with BC stimulation (Table 1).

In numerical studies on the inner ear, the RW membrane with a flat surface was modelled assuming isotropic and linear elastic properties [5], [6], [13], [14]. Viscoelastic properties were also considered for the flat RW surface, assuming the standard linear solid model, and a good agreement was achieved between numerical results and the experiment [7]. In the presented model, the RW membrane surface was convex like in a real cochlea, although it had only one curvature (Fig. 2b). The area of the RW membrane

Table 1. Tissue properties used for the finite element (FE) model

Tissue	Data	Reference
Compact bone	E_c' (Eq. (5)), E_c'' (Eq. (6)) $\nu_c = 0.3$ $\rho_c = 1.8$ g/cm^3	[17] [20]
Trabecular bone	$E_t = 87$ MPa $\nu_t = 0.3$ $\beta_t = 4.4563 \cdot 10^{-5}$ s $\xi_t = 0.056$ $\rho_t = 1.2$ g/cm^3	[21] [16] [21] [19]
Round window	E_r' (Eq. (7)), E_r'' (Eq. (8)) $\nu_r = 0.3$ $\rho_r = 1.2$ g/cm^3	[13] [7]
Basilar membrane	E_b (Eq. (9)) $\nu_b = 0.49$ $\beta_b = 1.27 \cdot 10^{-5}$ s, ξ_b (Eq. (10)) $\rho_b = 1.2$ g/cm^3	[13]
Spiral lamina	E_s (Eq. (11)) $\nu_s = 0.3$ $\beta_s = 0$ s, $\xi_s = 0.02$ $\rho_s = 2.2$ g/cm^3	
Spiral ligament	$E_l = 20$ MPa $\nu_l = 0.49$ $\beta_l = 0$ s, $\xi_l = 0.05$ $\rho_l = 1.2$ g/cm^3	[23] [6]
Stapes	$E_f = 17100$ MPa $\nu_f = 0.3$ $\beta_f = 1.6 \times 10^{-4}$ s, $\xi_f = 0$ $\rho_f = 2.3$ g/cm^3	[14]
Annular ligament	$E_a = 4$ MPa $\nu_a = 0.49$ $\beta_a = 1.3 \times 10^{-5}$ s, $\xi_a = 0.0918$ $\rho_a = 1.2$ g/cm^3	[23] [6]
Perilymph fluid	$K = 2150$ MPa $c = 1469$ m/s $\eta = 6.98 \times 10^{-4}$ Ns/m^2 $\rho = 0.994$ g/cm^3	[14]

Note: E – Young's modulus, E' – storage modulus, E'' – loss modulus, K – bulk modulus, ν – Poisson's ratio, ρ – density, coefficients of structural damping: β – frequency-dependent, ξ – frequency-independent, η – dynamic viscosity, c – speed of sound

was 2.49 mm^2 and the thickness was 0.07 mm. The RW membrane was modelled as a viscoelastic material, and the storage and loss moduli were tuned to meet two criteria. The first was the displacement amplitude measured by Asai et al. [1] at the center of the RW in the normal direction, for the entire frequency range from 0.2 to 10 kHz. The second criterion was related to the vibration modes shown in [26] for frequencies of 1, 2.5, 6, and 10 kHz. Numerical results were compared to the experimental data to get similar mode shapes. The storage E_r' and the loss E_r'' moduli (Eq. 7, 8) were dependent on the frequency f (Hz), and a was $\log_{10}(f)$.

$$E_r' = 2.57 \cdot 10^{\frac{-0.52}{1+0.86 \cdot \exp(3.4 \cdot 10^{-3} \cdot f - 6.936)}} + 5.02 \cdot 10^{-16} \cdot f^4 - 1.229 \cdot 10^{-11} \cdot f^3 + 9.173 \cdot 10^{-8} \cdot f^2 - 1.0 \cdot 10^{-4} \cdot f + 8.254 \cdot 10^{-2} \quad \text{[MPa]}, \tag{7}$$

$$E_r'' = -1.9814 \cdot a^5 + 30.245 \cdot a^4 - 181.204 \cdot a^3 + 535.378 \cdot a^2 - 784.403 \cdot a + 459.35 \quad \text{[MPa]}. \tag{8}$$

The BM is a complex anisotropic structure with the nonlinear stiffness. In the active model of the cochlea, the magnitude of vibration on the BM is amplified due to the presence of living outer hair cells. In this study, the passive linear behavior of the BM was assumed with no cochlear amplification, similarly as in the previous numerical simulations [6], [14]. The length of BM was 29.36 mm, the width was defined as a function of distance measured along the cochlea (Fig. 2f), from 0.074 mm at the base to 0.5 mm at the apex [4], and the thickness was assumed as 0.093 mm. The validation of the BM was performed based on experimental data. The criteria included the position of maximum vibration of the BM as a function of frequency according to [8] and the displacement amplitude and phase of a travelling wave at the selected point located 12 mm from the RW [9], [24]. The Young's modulus of the BM was set as an exponential function of the distance s measured from its base (Eq. (9)). The damping consisted of a frequency independent coefficient defined as an exponential function of the distance s (Eq. (10)), and a frequency dependent part constant along the BM (Table 1).

$$E_b = 10^{-(0.08863 \cdot s + 0.39794)} \quad \text{[MPa]}, \tag{9}$$

$$\xi_b = 0.2 \cdot 10^{\frac{0.55}{1+0.16 \cdot \exp(9.89 - 0.43 \cdot s)}}. \tag{10}$$

The SL structure is anisotropic due to the presence of nerve fibers. Based on CT imaging, it was difficult to determine the boundary between the flexible part of the SL and its stiffer base (Fig. 2f). It is known, that the properties of the SL significantly affect vibrations of the BM [23]. Too high stiffness of the SL, especially in the region close to the basal part of the cochlea, resulted in decreased amplitude and phase delay on the BM. The base of the SL was modeled as a compact bone forming the outer contour of the modiolus (Fig. 2h). For the flexible part of the SL, a linear isotropic material was used, with the Young's modulus changing along the cochlea (Eq. (11)), and with the frequency independent damping (Table 1).

$$E_s = 20 \cdot 10^{\frac{3.16}{1+6.3 \cdot \exp(0.475 \cdot s - 4.465)}} \text{ [MPa]}. \quad (11)$$

The only part of the middle ear included in the presented model was the stapes (Fig. 2a, e). The lack of the remaining ossicles, muscles, and ligaments was replaced by restoring all movements at the SF including piston-like and rocking motions [22]. The stapes was modelled using a linear isotropic material, with frequency-dependent damping (Table 1).

The annular ligament limits the SF movement and thus protects the cochlea. The spiral ligament participates in dynamic processes in the cochlea. Both tissues were modelled using a linear elastic, isotropic, and nearly incompressible material [23]. The thickness of the annular ligament was 0.16 mm and the width of the spiral ligament was about 0.4 mm. When the model was stimulated by the SF movement, the annular ligament was flexible. The Young's modulus and frequency – independent and – dependent damping coefficients were tuned during validation (Table 1). Too high stiffness of the annular ligament resulted in decreased amplitudes on the RW and BM. Similarly, the amplitude drop was also observed for too low stiffness and damping properties, due to opposite vibration phases of the stapes and the annular ligament. The spiral ligament had only the frequency-dependent part of damping (Table 1).

The fluid in the scala vestibuli and tympani and in the semicircular canals was modeled as viscous and compressible. A helicotrema with a cross–section of 0.14 mm^2 was included at the ending of scale (Fig. 2d). The Raisner's membrane was neglected due to its small thickness, so only one type of the cochlear fluid was considered – a perilymph. Because the fluid flow was not considered, the dynamic viscosity was used only for the vibration damping (Table 1). A slight energy dissipation at the interface between the fluid and structure was included as the boundary admittance of 0.008, chosen from the range of 0 to 1 during validation of the cochlea.

2.3. FE analyses

Numerical simulations of the FE model were performed using the ANSYS17.2 program (ANSYS Inc., Canonsburg, Pennsylvania, United States). After verification (model continuity, material properties assignment, mesh density, numerical integration schemes, distortion criteria), the model was validated based on experimental data. Harmonic analyses were performed for 17 frequencies from the hearing range (0.2, 0.3, 0.4, 0.5, 0.63, 0.8, 1.0, 1.25, 1.6, 2.0, 2.5, 3.15, 4.0, 6.0, 6.3, 8 and 10 kHz) [13]. The temporal bone was supported by fixing the displacements on the surfaces connected with adjacent skull bones (sphenoid, occipital, parietal, and zygomatic) (Fig. 3b). The outer surface (area of 10 040 mm^2 – inside and outside the skull) was covered by uniformly distributed mass, imitating soft tissues near the tempotal bone. The surface density value has been adjusted during validation to 0.0025 g/mm^2.

The two different types of harmonic load were considered. The FE model with the SF movement imi-

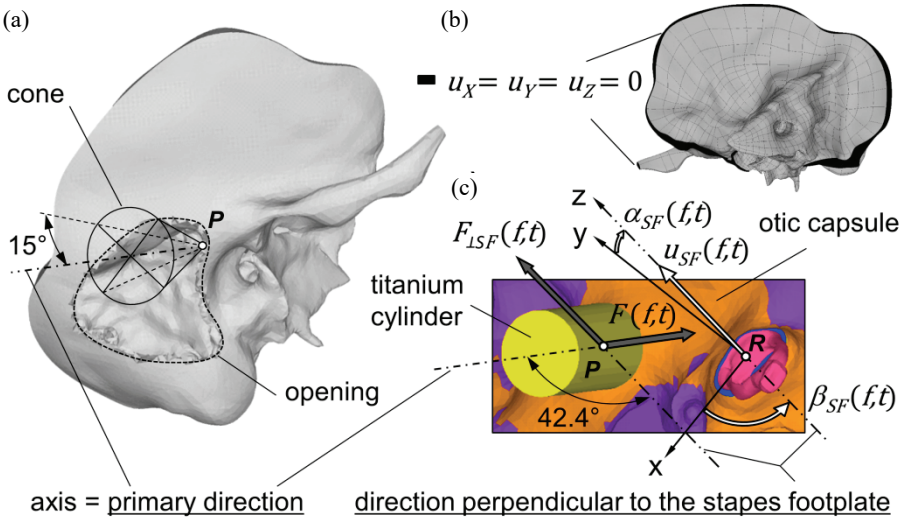

Fig. 3. Finite element (FE) model assumptions; (a) an imaginary cone inscribed in the typical opening performed during mastoidectomy – the axis of the cone determined the primary direction of the force for bone conduction (BC) stimulation, (b) fixed support of the bone boundary, (c) applied loads: the two forces for BC stimulation and the movement of the stapes footplate (SF) for air conduction (AC) stimulation – the z axis was perpendicular to the SF

tating the AC pathway was used to validate the cochlea, and as the reference for BC stimulation. The stimulation included translation of the SF in the perpendicular direction (z), and rotations along the long (x) and short (y) axes (Fig. 3c). A harmonic function of translation $u_{SF}(f, t) = A_{SF}(f)\cdot\sin(2\pi ft)$ was applied at a single node located at point R and coupled to the nodes located on the SF outer surface by using multipoint constraints. The displacement amplitudes $A_{SF}(f)$ were based on experimental measurements for the sound pressure level of 80 dB [1]. A positive value of $u_{SF}(f, t)$ denoted squeezing the stapes into the oval window. The amplitudes and phases of rotations $\alpha_{SF}(f, t)$ and $\beta_{SF}(f, t)$ were recalculated from rotational velocities, experimentally measured and normalized by the ear-canal pressure by Sim et al. [22]. The phases of rotations corresponded to the phase of translation $u_{SF}(f, t)$.

The FE model stimulated by a harmonic force imitating the BC pathway was initially used to validate the temporal bone properties. However, the main target was to find the value of force needed for BC stimulation applied on the otic capsule, and to investigate the effect of the stimulation direction. BC analysis was performed for two directions of the force applied on the otic capsule. The primary direction was coincident with the axis of an imaginary cone, inscribed in the typical opening performed during mastoidectomy (Fig. 3a). The apex of the cone was located on the otic capsule surface above the lateral semicircular canal (point P). The second direction was perpendicular to the SF and was tilted forward from the axis of the cone (Fig. 3c). The BC stimulator was assumed as a titanium cylinder with diameter of 3 mm, height of 5 mm, and density of 4.5 g/cm^3 (Fig. 3c). The mass of the stimulator was concentrated in a single node located at point P and coupled to the nodes lying on the otic capsule surface under the base of the cylinder. A harmonic function of force $F(f, t) = F_{\perp SF}(f, t) = F_a \sin(2\pi f\cdot t)$ was applied at point P. The force amplitude F_a = 0.1 N was assumed as constant for the entire frequency range, similarly as in the experiment conducted on cadavers by Kwacz et al. [15]. The positive force value was directed toward the otic capsule. For BC stimulation, the two conditions were considered regarding the stapes movement. The first was a free stapes, when the annular ligament was assumed as flexible (Table 1). The second was the immobilized SF (otosclerotic condition), when the properties of the annular ligament were replaced by compact bone.

Nodal displacements of solid tissues were determined as complex numbers. The absolute values of amplitudes and phases were based on the real and imaginary part of the solution. The relative amplitudes were determined by subtracting the vibration of the surrounding bone from the vibration of the flexible tissue. For the RW membrane, the vibration direction perpendicular to the surface at point C was considered (Fig. 2b). The relative amplitude at the RW center was calculated as the average value based on the promontory vibration at points A and B (Eq. (12)).

$$A_C^{rel} = \frac{1}{2}\left(\sqrt{(u_C^{Re} - u_A^{Re})^2 + (u_C^{Im} - u_A^{Im})^2} + \sqrt{(u_C^{Re} - u_B^{Re})^2 + (u_C^{Im} - u_B^{Im})^2}\right). \tag{12}$$

The volume displacement (VD) on the RW membrane was calculated as a complex number, using the procedure described in [24]. Assuming rigid body motion of the promontory, 48 points located on the RW perimeter were used to determine the averaged movement of the bone, including translation in the direction perpendicular to the RW surface at its center, and rotations about the two axes shown as dashed lines in Fig. 2b. The real and imaginary part of the promontory movement was then subtracted from the displacement of the RW surface in the normal direction, to get the relative displacement. In the presented model, the RW surface was divided by 436 triangles having vertices in nodal points belonged to the surface. The relative displacement at the centroid of each triangle was multiplied by its surface, and then summarized to calculate the VD.

In each cross-section of the cochlea (Fig. 2g), the three characteristic points were chosen to calculate the relative displacement amplitudes in the direction parallel to the modiolus axis: point E on the SL edge and point F – on the BM. The relative displacement amplitudes on the SL edge and the BM center (Eq. (13)) were based on the displacement at point D. The distance between the two neighboring cross-sections was about 0.06 to 0.14 mm.

$$A_i^{rel} = \sqrt{(u_i^{Re} - u_D^{Re})^2 + (u_i^{Im} - u_D^{Im})^2}; \quad i = E, F. \tag{13}$$

The relative amplitudes were also used to scale the force amplitude for BC stimulation at a given frequency, so that the displacement amplitude was close to the result of AC stimulation applied on the SF. Force F_{RW} regarding the vibration on the RW membrane center was based on the applied load F_a and relative displacements (Eq. (12)), respectively for AC and BC stimulation (Eq. (14)). For the entire RW

membrane, force F_{VD} was based on VD amplitudes (Eq. (15)).

$$F_{RW} = \frac{A_C^{rel}(AC)}{A_C^{rel}(BC)} \cdot F_a, \tag{14}$$

$$F_{VD} = \frac{VD(AC)}{VD(BC)} \cdot F_a. \tag{15}$$

Force amplitudes were also scaled regarding the BM center and the SL edge, based on the relative displacements from the Eq. (13). The entire number of cross-sections along the cochlea was 317, but the sum was calculated over a smaller number n, to exclude the cross-sections, where the relative amplitudes obtained for BC stimulation were close to zero (Eqs. (16) and (17)).

$$F_{BM} = \frac{F_a}{n} \sum_{i=1}^{n} \frac{A_F^{rel}(AC)_i}{A_F^{rel}(BC)_i}, \tag{16}$$

$$F_{SL} = \frac{F_a}{n} \sum_{i=1}^{n} \frac{A_E^{rel}(AC)_i}{A_E^{rel}(BC)_i}. \tag{17}$$

3. Results

3.1. AC stimulation applied to the SF

The amplitude of the RW displacement for AC stimulation was the highest at its center for nearly entire frequency range except for 4 and 5 kHz (Fig. 4a). The differences between the phase angles of selected points were increasing along with frequency (Fig. 4b), relatively to the vibration mode changes (Fig. 4a). At low frequencies, the phase of the RW displacement was opposite to the SF translation phase. The mode shape was almost constant below 1 kHz (Fig. 4a).

The magnitude ratio of the BM displacement (Fig. 5a) was calculated along of the cochlea as the $20\log_{10}(A_F(s,f)/A_{SF}(f))$, where $A_F(s,f)$ was the displacement amplitude at point F in each cross-section (Fig. 2g), and $A_{SF}(f)$ was the displacement amplitude applied on the SF for a given frequency. The position of maximum vibration on the BM was compared with

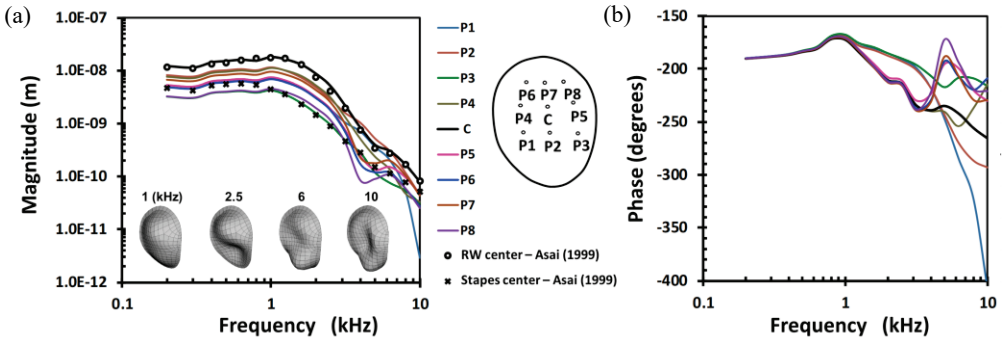

Fig. 4. Vibration of the round window (RW) membrane for air conduction (AC) stimulation applied on the stapes footplate (SF): (a) the absolute displacement amplitudes at 9 points located on the RW surface compared to the experiment [1], the mode shapes for selected frequencies (phase about 0.25 of the vibration period), (b) phases calculated relatively to the SF vibration

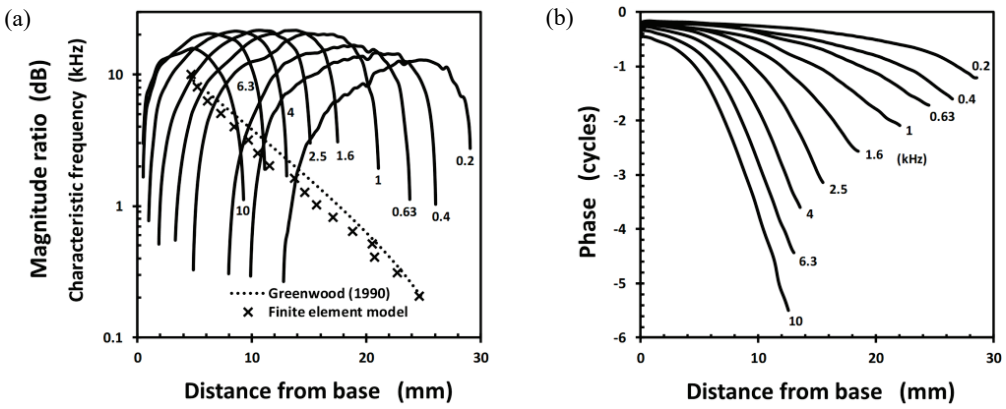

Fig. 5. Vibration of the basilar membrane (BM) for air conduction (AC) stimulation applied on the stapes footplate (SF) along the cochlea: (a) the ratio of the absolute displacement amplitude on the BM to the translation applied on the SF, and the characteristic frequencies (crosses) compared with [8] (dashed line), (b) an accumulated phase of the BM displacement

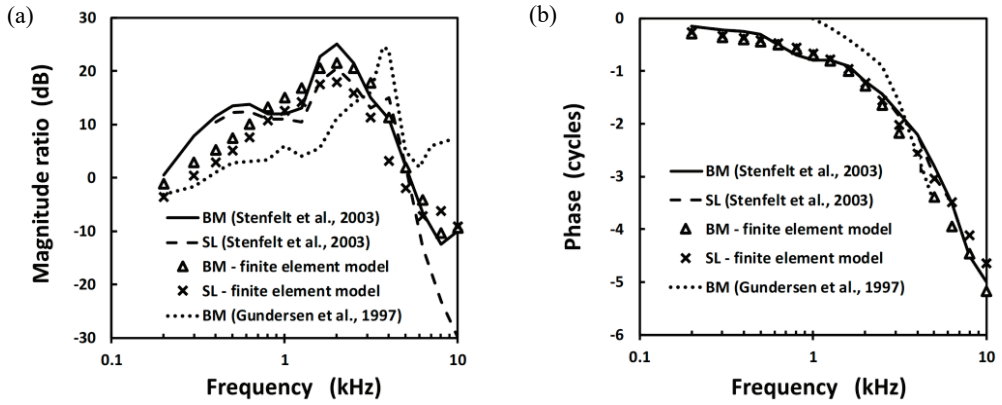

Fig. 6. Vibrations of the basilar membrane (BM) and the spiral lamina (SL) edge in the cross-section located 12 mm from base, for air conduction (AC) stimulation applied on the stapes footplate (SF): (a) ratios of the absolute displacement amplitudes on the BM and the SL edge, related to the translation applied on the SF, (b) accumulated phases of displacements on the BM and the SL edge

the Greenwood function [8], where a characteristic frequency was defined as the frequency providing the maximum displacement amplitude at a given point along the BM length (Fig. 5a).

At low and high frequencies, numerical results agreed with the Greenwood function [8]. For other frequencies, the position of maximum vibration was slightly shifted towards the base of the cochlea. An accumulated phase on the BM was shown for the distance range, where the travelling wave occurred (Fig. 5b). The BM and SL vibrations in the cross-section located 12 mm from base were compared to experimental data [9], [24]. The magnitude ratio of the SL displacement was calculated as the $20\log_{10}(A_E(s,f)/A_{SF}(f))$, where $A_E(s,f)$ was the displacement amplitude at point E. For the presented model, the course of the magnitude ratio for the entire frequency range was similar as measured by Stenfelt et al. [24], although the numerical results were underestimated at low frequencies (Fig. 6a). Phases were close to the experimental data [24] and similar for the BM and the SL edge (Fig. 6b).

3.2. BC stimulation applied on the otic capsule

The results of the VD on the RW membrane for BC stimulation assuming the model with the free stapes were close to obtained for the immobilized stapes at low frequencies up to 0.8 kHz, and then smaller because of opposite vibration phases on the SF and the RW membrane (Fig. 7a). The VD for the model with the free stapes was close to the experimental data [15] at 0.5 kHz and above 2 kHz. Results of AC stimulation were comparable with [25], considering that those measurements were performed for male specimens with greater size of the SF and the RW, compared with the female temporal bone used in this study. For BC stimulation and low frequencies, the force amplitude of 0.1 N provided similar value of the VD as for AC stimulation. For the frequencies above 0.8 kHz the force magnitude was too high. The phase courses were similar, although more irregular for BC stimulation with the free stapes (Fig. 7b).

The promontory displacement was not depending on the stapes mobility (Figs. 8a, b). The numerical results of BC stimulation were close to those obtained experimentally ([15]) except for 2.5 kHz and were about three orders of magnitude greater than obtained for AC stimulation.

For the FE model with the immobilized stapes, the force amplitudes needed for BC stimulation were calculated according to Eqs. (14)–(17) (Fig. 9). The forces for the primary direction (Fig. 9a) were lower than for the direction perpendicular to the SF (Fig. 9b). It was interesting, that the course of the force amplitude for the primary direction was like the course of the translation applied on the SF for AC stimulation (Fig. 4a). The ratio of $F_{VD\perp SF}(f)/F_{VD}(f)$ was about 4 up to 0.4 kHz, decreased to 1 at 0.8 kHz, remained constant to 2.5 kHz, increased to about 7 at 5 kHz, and was constant up to 10 kHz. The course of $F_{RW\perp SF}(f)/F_{RW}(f)$ was similar as for the VD. The ratio of $F_{BM\perp SF}(f)/F_{BM}(f)$ was about 5 up to 1.25 kHz, rapidly decreased to 1 at 1.6 kHz, was constant to 2.5 kHz, increased to 3.5 at 4 kHz, and then was constant. The course of $F_{SL\perp SF}(f)/F_{SL}(f)$ was similar as for the BM, except 0.2 and 0.63 kHz. The discrepancy between the force amplitudes needed for excitation of the RW and the BM was much greater, if the force direction was perpendicular to the SF.

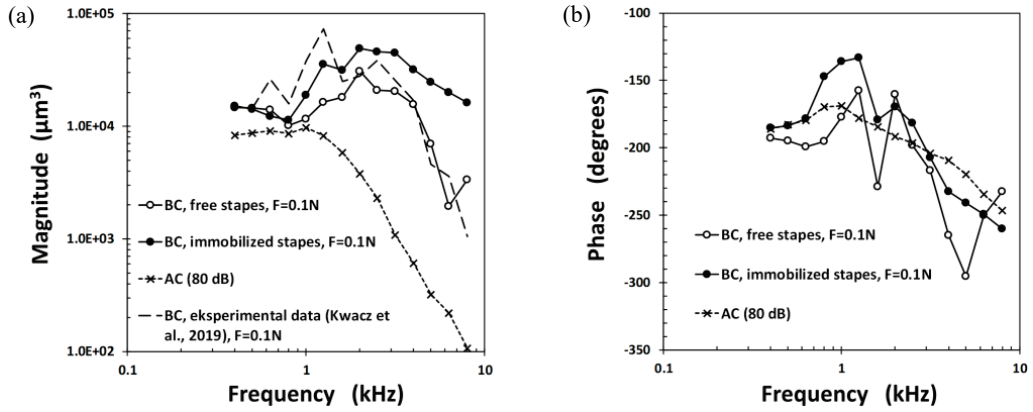

Fig. 7. The volume displacement (VD) of the round window (RW) membrane:
(a) amplitude, (b) phase. Numerical results compared with the experiment by Kwacz et al. [15].
AC, BC – air and bone conduction stimulation

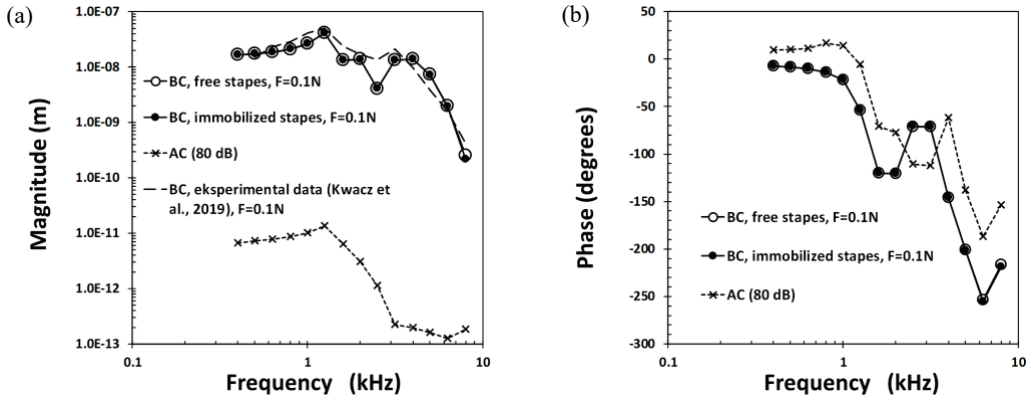

Fig. 8. The promontory displacement in the direction perpendicular to the round window (RW):
(a) amplitude, (b) phase. Numerical results compared with the experiment by Kwacz et al. [15].
AC, BC – air and bone conduction

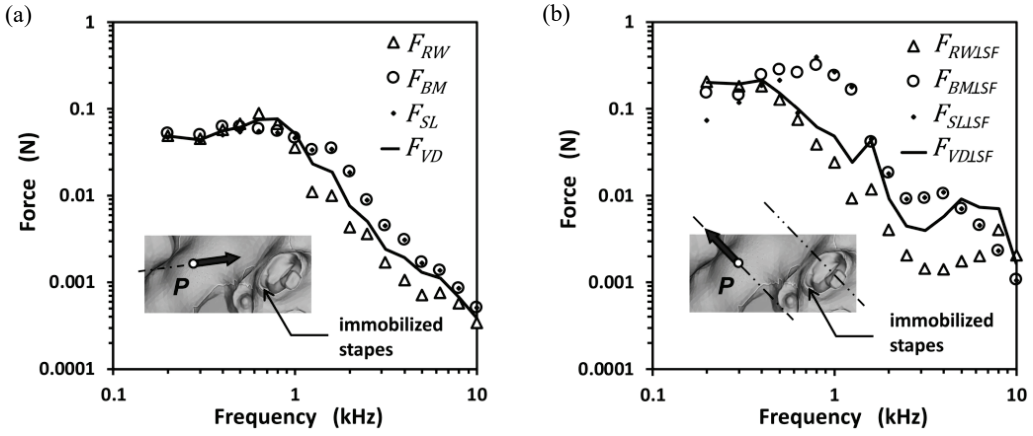

Fig. 9. Amplitudes of harmonic forces for bone conduction (BC) stimulation
applied on the otic capsule resulting in similar results as obtained for air conduction (AC) stimulation:
(a) the force in the primary direction, (b) the force in the direction perpendicular to the stapes footplate (SF)

Vibration of the BM for AC stimulation applied on the SF was compared to the two directions of BC stimulation, applied on the otic capsule, and assuming the immobilized stapes (Fig. 10). The force amplitudes $F_{VD}(f)$ and $F_{VD\perp SF}(f)$ were calculated from the Eq. (15), to get the same values of the VD on the RW

membrane, as were obtained for AC stimulation. The harmonic force for the primary direction was set as $F_{BC}(f, t) = F_{VD}(f) \sin(2\pi ft)$, and the force for the direction perpendicular to the SF was $F_{BC\perp SF}(f, t) = F_{VD\perp SF}(f) \sin(2\pi ft)$.

The real and imaginary parts of displacements along the BM were used to calculate the absolute envelope of vibration. The relative envelope was based on the relative displacement amplitude at point F in each cross-section (Eq. (13)), regarding the vibration of the SL base. For AC stimulation, the vibration of the bone was not significant for all frequencies, and, consequently, the relative and absolute envelopes were nearly the same. For the primary direction of BC stimulation at low frequencies (0.2 and 1 kHz), the displacement amplitudes of the SL base significantly influenced the BM vibration. Above 2.5 Hz, the displacement of the SL base was not significant. The shape of the relative envelope for the primary direction was similar as for AC stimulation, although the magnitude at 2.5 Hz was about two times greater. For the force direction perpendicular to the SF, the displacement of the bone at low frequencies was several times greater than for the primary direction, and the shape of the relative envelope was different than for AC stimulation. At high frequencies of 6.3 and 10 kHz, the magnitude of the relative envelope was greater for BC⊥SF stimulation, and the shape was similar as for AC stimulation. Position of the maximum vibration of the BM was closer to the theory [8] for the primary direction, compared to the direction perpendicular to the SF (Fig. 10).

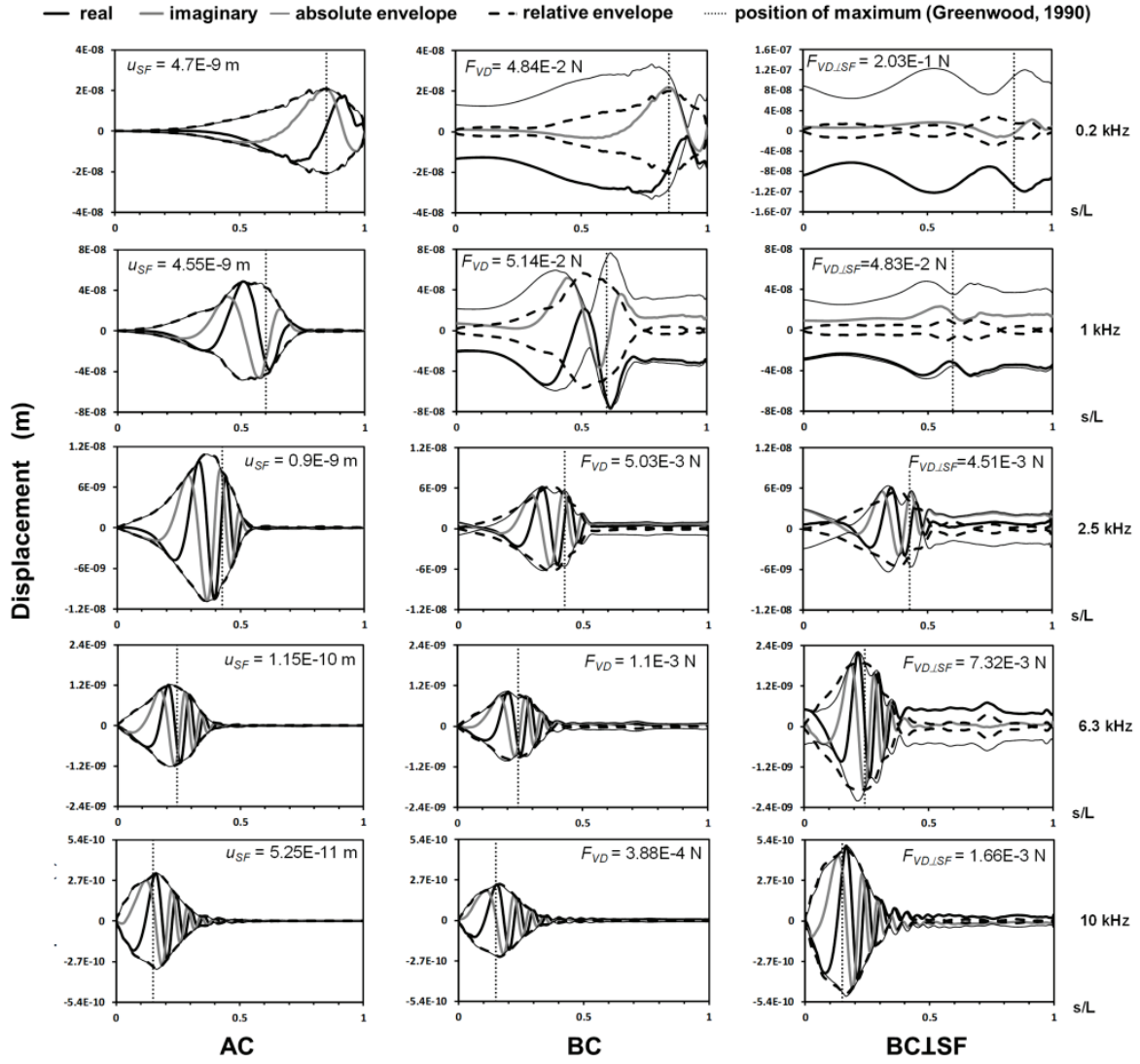

Fig. 10. Vibration of the basilar membrane (BM) as a function of the normalized distance along the cochlea, for air conduction (AC) stimulation and the two directions of bone conduction (BC) stimulation: primary and perpendicular to the stapes footplate (SF). The finite element (FE) model with the immobilized stapes was considered for BC stimulation

4. Discussion

The presented FE model was used to supplement experimental studies, which in the case of patient studies, in addition to ethical regulations, are limited by the patient's time under anesthesia and difficulties in access to the examined place, usually performed by violation of adjacent tissues. Thus, the use of numerical modelling was justified, considering that it was closely related to the parallelly conducted experimental research [15].

The force amplitudes obtained from FE analysis may be used to adjust the power of the BC stimulator. The results of this study showed the direction of the force applied on the otic capsule to be an important factor determining the effectiveness of BC stimulation. This issue should be further investigated to find the optimal direction for the entire frequency range.

As shown in this study, the dynamic response of the structure strongly depended on the mass and stiffness distribution. Although the shape of the temporal bone was reconstructed as precisely as possible, is was difficult to model the large scatter of the bony tissue properties. To determine the bone contour, a certain threshold on the gray scaled CT images was set, but the heterogeneity of the structure was not considered. At the FE model processing, the region of cortical bone was approximately determined by selecting the subsequent layers of finite elements. Nevertheless, the model was well fitted to the experimental data (Fig. 8). Beside the stiffness and mass distribution, the resonance frequencies of the structure also depended on boundary conditions. In the presented model, the temporal bone border was fixed assuming that the skull adjacent to the temporal bone has infinite stiffness, which resulted in overestimated resonance frequencies. This effect was compensated by adjusting the mass of soft tissues on the temporal bone surface. The first resonance frequency for the entire skull reported by Håkansson et al. [10] was about 0.8 kHz, so the fixed displacement on the border seems to be acceptable only for the BC stimulation applied on the otic capsule, but not on the squamous part.

In this study, the passive cochlear model was used, because the cochlea was validated based on experimental tests on cadavers [1], [24], [26]. Further research is needed to find out, how the response of the cochlea for BC stimulation would be influenced by cochlear amplification. Validation of the cochlea was an iterative process, because the vibration of the RW membrane also depended on the BM properties as well as the BM properties required considering flexibility of the SL. The shape of the RW membrane was smoothed, so the mode shapes from numerical analysis did not exactly match other experimental results [26]. However, the maximum vibrations on the RW membrane center were adjusted to decrease the difference between the numerical and experimental results to ±10%. It should be mentioned that larger spread of results between specimens was observed in the test [1]. In the presented model, location of the maximum amplitude on the BM was determined for the vibration direction parallel to the modiolus axis, while the BM had the helical shape with a variable slope, so that the results may be slightly different, compared with the theory [8]. The middle and outer ear structures were not included in the presented FE model, and for BC stimulation, the stapes were assumed as free or immobilized. The analyzed otosclerotic condition (immobilized stapes) mimicked the conductive component of hearing loss, and we believe that the results obtained in this condition are of practical importance, however, further research is needed.

5. Conclusions

The cochlear response for BC stimulation was comparable with the result obtained for AC stimulation. The forces amplitudes needed for BC stimulation were changing with frequency and depended on the direction. The optimal direction of BC stimulation applied on the otic capsule was not coincident with the direction perpendicular to the stapes footplate. The effectiveness of BC stimulation was higher when the force was more oriented towards the cochlea. The primary direction (coincident with the axis of an imaginary cone) was chosen because of its availability during mastoidectomy, however, it was also advantageous compared to the direction perpendicular to the stapes footplate, because of the smaller force amplitude needed for BC stimulation. Due to the small thickness of compact bone in the proximity of the lateral semicircular canal, a different site of BC stimulation should also be considered.

Acknowledgement

This work was supported by the National Centre for Research and Development grant number PBS3/B7/25/2015.

References

[1] ASAI M., HUBER A.M., GOODE R.L., *Analysis of the best site on the stapes footplate for ossicular chain reconstruction*, Acta Otolaryngol. (Stockh.), 1999, 119 (5), 356–361.

[2] CHANG Y., KIM N., STENFELT S., *The development of a whole--head human finite element model for simulation of the transmission of bone-conducted sound*, J. Acoust. Soc. Am., 2016, 140, 1635–1651.

[3] EEG-OLOFSSON M., STENFELT S., TAGHAVI H., HÅKANSSON B., TENGSTRAND T., FINIZIA C., *Transmission of bone conducted sound – Correlation between hearing perception and cochlear vibration*, Hear Res., 2013, 306, 11–20.

[4] FERNANDEZ C., *Dimensions of the Cochlea (Guinea Pig)*, J. Acoust. Soc. Am., 1952, 24, 519–522.

[5] GAN R.Z., SUN Q., FENG B., WOOD M.W., *Acoustic-structural coupled finite element analysis for sound transmission in human ear – Pressure distributions*, Med. Eng. Phys., 2006, 28, 395–404.

[6] GAN R.Z., REEVES B.P., WANG X., *Modeling of Sound Transmission from Ear Canal to Cochlea*, Ann. Biomed. Eng., 2007, 35 (12), 2180–2195.

[7] GAN R.W., ZHANG X., *Dynamic Properties of Human Round Window Membrane in Auditory Frequencies*, Med. Eng. Phys., 2013, 35 (3), 310–318.

[8] GREENWOOD D.D., *A cochlear frequency-position function for several species-29 years later*, J. Acoust. Soc. Am., 1990, 87, 2592–2605.

[9] GUNDERSEN T., SKARSTEIN O., SIKKELAND T., *A study of the vibration of the basilar membrane in human temporal bone preparations by the use of the Mössbauer effect*, Acta Otolaryngol., 1997, 86 (1978), 225–232.

[10] HÅKANSSON B., BRANDT A., CARLSSON P., TJELLSTRÖM A., *Resonance frequencies of the human skull in vivo*, J. Acoust. Soc. Am., 1994, 95 (3), 1474–81.

[11] HÅKANSSON B.E., EEG-OLOFSSON M., REINFELDT S., STENFELT S., GRANSTRÖM G., *Percutaneous versus transcutaneous bone conduction implant system: a feasibility study on a cadaver head*, Otol. Neurotol., 2008, 29, 1132–1139.

[12] JOHNSON T.P.M., SOCRATE S., BOYCE M.C., *A viscoelastic, viscoplastic model of cortical bone valid at low and high strain rates*, Acta Biomater., 2010, 6, 4073–4080.

[13] KWACZ M., MAREK P., BORKOWSKI P., MRÓWKA M., *A three-dimensional finite element model of round window membrane vibration before and after stapedotomy surgery*, Biomech. Model Mechanobiol., 2013, 12(6), 1243–61.

[14] KWACZ M., MAREK P., BORKOWSKI P., GAMBIN W., *Effect of different stapes prostheses on the passive vibration of the basilar membrane*, Hear Res., 2014, 310, 13–26.

[15] KWACZ M., NIEMCZYK K., WYSOCKI J., LACHOWSKA M., BORKOWSKI P., MAŁKOWSKA M., SOKOŁOWSKI J., *Round Window Membrane Motion Induced by Bone Conduction Stimulation at Different Excitation Sites: Methodology of Measurement and Data Analysis in Cadaver Study*, Ear Hearing., 2019, Apr. 4, DOI: 10.1097/AUD.0000000000000725.

[16] LAKATOS E., MAGYAR L., BOJTÁR I., *Material Properties of the Mandibular Trabecular Bone*, Journal of Medical Engineering, 2014, DOI: 10.1155/2014/470539.

[17] LAKES R.S., *Dynamic study of couple stress effect in human compact bone*, J. Biomech. Eng., 1982, 104 (1), 6–11.

[18] LIU H., XU D., YANG J., YANG S., CHENG G., HUANG X., *Analysis of the influence of the transducer and its coupling layer on round window stimulation*, Acta Bioeng. Biomech., 2017, 19 (2), 103–111.

[19] OUYANG J., YANG G.T., WU W.Z., ZHU Q.A., ZHONG S.Z., *Biomechanical characteristics of human trabecular bone*, Clin. Biomech., 1997, 12 (7–8), 522–524.

[20] PETERSON J., DECHOW P.C., *Material Properties of the Inner and Outer Cortical Tables of the Human Parietal Bone*, Anat. Rec., 2002, 268, 7–15.

[21] RONCA D., GLORIA A., DE SANTIS R., RUSSO T., D'AMORA U., CHIERCHIA M., NICOLAIS L., AMBROSIO L., *Critical analysis on dynamic-mechanical performance of spongy bone: the effect of acrylic cement*, Hard Tissue, 2014, May 11, 3 (1), 9.

[22] SIM J.H., CHATZIMICHALIS M., LAUXMANN M., RÖÖSLI CH., EIBER A., HUBER A.M., *Complex Stapes Motions in Human Ears*, Jaro, 2010, 11, 329–341.

[23] SONG Y, DEBSKI RE, MUSAHL V, THOMAS M, WOO S.L., *A three-dimensional finite element model of the human anterior cruciate ligament: a computational analysis with experimental validation*, J. Biomech., 2004, 37, 383–390.

[24] STENFELT S., PURIA S., HATO N., GOODE R.L., *Basilar membrane and osseous spiral lamina motion in human cadavers with air and bone conduction stimuli*, Hear Res., 2003, 181 (1–2), 131–43.

[25] STENFELT S., HATO N., GOODE R.L., *Fluid volume displacement at the oval and round windows with air and bone conduction stimulation*, J. Acoust. Soc. Am., 2003, 115 (2), 797–812.

[26] STENFELT S., HATO N., GOODE R.L., *Round window membrane motion with air conduction and bone conduction stimulation*, Hear Res., 2004, 198 (1–2), 10–24.